ENERGY LEVEL SCHEME OF Nd^{3+} ION IN RARE EARTH OXYHALIDES, REOX (X = F, Cl, AND Br)*

L. BEAURY[a], J. HÖLSÄ[b], J. KORVENTAUSTA[b], J.-C. KRUPA[c], R.-J. LAMMINMÄKI[b], P. PORCHER[a], H. RAHIALA[d] AND E. SÄILYNOJA[b]†

[a]C.N.R.S., U.P.R. 209, F-92195 Meudon, France
[b]University of Turku, Department of Chemistry, FIN-20014 Turku, Finland
[c]I.P.N., Laboratoire de Radiochimie, F-91406 Orsay, France
[d]Åbo Akademi University, Department of Chemistry, FIN-20500 Turku, Finland

(Received June 24, 1996)

The energy level schemes of the neodymium oxyhalides (NdOX, X = F, Cl, and Br) were studied and simulated with a phenomenological model accounting simultaneously for both the free ion interactions and the crystal field effect. The former included the electrostatic and interconfigurational interactions as well as the spin–orbit coupling. The simulations were carried out by using the data from the optical absorption and luminescence as well as the inelastic neutron scattering measured at low temperatures between 2.5 and 77 K. The values of the Slater integral F^2 describing the electrostatic interactions decrease while F^4 and F^6 increase as a function of the ionic radius of the halide anion. The strength of the spin–orbit coupling is quite the same in all three matrices. The crystal field effect — measured as the crystal field strength parameter S — is almost twice as strong in the hexagonal NdOF matrix (650 cm^{-1}) than in the tetragonal NdOCl or NdOBr (367 and 378 cm^{-1}, respectively). Similar evolution was obtained for the short- and mid-range crystal field strengths related to the spatial extension of the interaction.

PACS numbers: 71.55.–i, 71.70.Ch, 78.40.–q, 78.55.–m

1. Introduction

The $4f$ orbitals of the trivalent rare earth (RE) ions are well protected from the ligand interaction by the filled $6s$ and $5p$ orbitals. The chemical properties of the trivalent RE ions vary hence little from one ion to another, but the filling of the $4f$ orbital plays an important role in the optical and magnetic properties of

*This paper has been presented at the 2nd Winter Workshop on Spectroscopy and Structure of Rare Earth Systems, Polanica Zdrój, Poland, 1996.

†Corresponding author.

RE compounds. Due to the shielding effect, only small shifts in the positions of the energy levels are observed from one host matrix to another. The crystal field (c.f.) effect is the main factor responsible for the differences in the spectroscopic properties of the same RE^{3+} ion in different matrix. This c.f. effect is considered as an action which breaks down the spherical symmetry of the free ion in the solid state [1–3]. The RE oxyhalides give an excellent opportunity to a systematic study of the changes in the optical properties of a given RE^{3+} ion when the matrix anion is changed.

The RE oxycompounds have the general formula $(REO)_nX$, where the anion X^{n-} can be almost any simple or complex ion. The structure comprises alternating layers of the complex cation $(REO)_n^{n+}$ and the anions [4]. The arrangement of the $(REO)_n^{n+}$ units leads to two types of the RE oxycompounds, one having a tetragonal symmetry due to a two-dimensional network of the ORE_4 units. In the other structural type, the ORE_4 units are linked three-dimensionally yielding trigonal symmetry [5].

The structure of the stoichiometric RE oxyfluorides, REOF, can be related to the fluorite structure, but is slightly distorted from cubic toward rhombohedral with $R\bar{3}m$ ($Z = 2$, No. 166 [6]) as the space group [7]. The distribution of the anions is also ordered. The RE^{3+} ion is eightfold coordinated to four oxygens and to four fluorides resulting in the C_{3v} point symmetry of the RE site. The coordination polyhedron around the RE atom is a fairly regular bicapped trigonal antiprism. The lighter RE oxychlorides, REOCl (RE = La–Ho), as well as all RE oxybromides have a tetragonal PbFCl-type structure [8–10] (space group $P4/nmm$ ($Z = 2$, No. 129 [6])). The RE^{3+} ion is coordinated to four oxygens and to four + one halides forming a monocapped tetragonal antiprism as the coordination polyhedron. The point symmetry of the RE site is C_{4v} [9].

In this paper, the experimental energy level schemes of the different neodymium oxyhalides were deduced from the optical absorption, luminescence and inelastic neutron scattering data and simulated with a phenomenological model. This model accounts simultaneously for the free ion and c.f. interactions. The evolution of these interactions was discussed in terms of the different effects involved, i.e. nephelauxetic effect and covalence. In addition, the energies of the individual Stark levels were studied in order to observe the correlation between them and the evolution of the free ion and/or the c.f. effects. The strength of the c.f. interaction was dealt with the strength parameters S, S^2, S^4, and S^6 to give a spatial extension of the c.f. effect.

2. Experimental details

2.1. Sample preparation

The polycrystalline RE oxyhalide samples were prepared by the solid state reaction between Nd_2O_3 and NH_4X (X = F, Cl, or Br). In order to obtain stoichiometric compounds the following experimental conditions were used: the NH_4X/Nd_2O_3 ratios 2.15, 2.15, and 2.5 and the reaction temperatures 1050, 950, and 900°C for NdOF, NdOCl, and NdOBr, respectively. The reaction time was always one hour. The preparation of the oxychloride and oxybromide samples was

carried out in static N_2 atmosphere in order to avoid the reaction back to Nd_2O_3. For the luminescence measurements the LaOX and GdOX (X = F and Cl) hosts were doped with one mole % of the Nd^{3+} ion. The NdOCl single crystals were used as well [11].

The routine X-ray powder diffraction analysis was used to verify the structure and purity of the RE oxyhalides. In all cases, no anomalous phases were observed.

2.2. Spectroscopic measurements

The luminescence spectra of the Nd^{3+} doped LaOX and GdOX (X = F and Cl) were recorded at 9 and 300 K in the NIR region between 887 and 943 nm. The luminescence was excited with the 457.9 nm line of a Carl Zeiss Jena ILA 120-1 argon ion laser and dispersed by a Carl Zeiss Jena GDM 1000 monochromator.

The optical absorption spectra of the NdOF and NdOBr samples were measured by using a Cary 5E UV-Vis-NIR spectrometer at selected temperatures between 9 and 300 K from 170 to 3300 nm. The instrument reproducibility was better than 2 Å and the band width was 0.6 Å. The samples were prepared by mixing NdOX to KBr and pressing a transparent disk. For NdOCl a Cary 17 spectrometer and the temperatures 4.2, 77, and 300 K were used [11].

The inelastic neutron scattering (INS) measurements on polycrystalline NdOF were carried out at ILL (Grenoble, France) by using an IN 4 time of flight (TOF) spectrometer at 2.5 K [12]. The low (average 10.2°) scattering angle was used for the measurements to avoid the interference from lattice vibrations.

3. Experimental results

3.1. Theoretical background

The principal interactions in the free ion electron structure of the RE^{3+} ions within the $4f^N$ configuration include the mutual Coulomb interaction between the $4f$ electrons (except for the $4f^1$ and $4f^{13}$ configurations) and the coupling of their spin and orbital angular momentum [13]. For accurate results, all the electrostatic interactions within and between the configurations should be included to the calculations. The configuration interactions have been taken into account by using the two- and three-body electrostatic terms [14]. In addition to the free ion interactions, the c.f. effect must be taken into account when dealing with the solid state. The RE ion experiences the c.f. effect as an inhomogeneous electrostatic field which is produced by the surrounding charge distribution [15].

The simulation of the energy level scheme of the $4f^3$ configuration was carried out by using a phenomenological model which treated simultaneously the free ion and c.f. effects. The effective free ion Hamiltonian H_{FI} is given by the following equation [13, 14]:

$$H_{\mathrm{FI}} = H_0 - \sum_{k=0,1,2,3} E_k(nf, nf)\mathrm{e}^k + \zeta_{4f} A_{\mathrm{SO}} + \alpha L(L+1)$$

$$+\beta G(G_2) + \gamma G(R_7) + \sum_{k=2,3,4,6,7,8} T^k t_k. \qquad (1)$$

H_0 is the spherical harmonic part. The Racah parameters, E_k ($k = 0$, 1, 2, and 3), are for the Coulomb repulsion between the $4f$ electrons. ζ_{4f} is a phenomenological parameter representing the spin–orbit interaction [13]. The two- and three-body interactions are parameterized by the Trees (α, β, and γ) and Judd (T^k ($k = 2$, 3, 4, 6, 7, and 8)) parameters [14]. The other symbols have their usual meaning [13,14].

The standard one-electron c.f. Hamiltonian H_{CF} is incorporated to the total Hamiltonian by the following equation:

$$H_{CF} = \sum_k \sum_{q=0}^{q=k} \{B_q^k [C_q^k + (-1)^q C_{-q}^k] + \mathrm{i} S_q^k [C_q^k - (-1)^{-q} C_{-q}^k]\}, \tag{2}$$

which gives the c.f. interaction as a sum of the products between the real B_q^k (or imaginary S_q^k) c.f. parameters and the spherical tensors C_q^k of rank k. The values of k and q are limited by the point symmetry of the RE site. In the case of the rather high C_{4v} (C_{3v}) site symmetry, the number of the c.f. parameters is restricted to five (six) real ones, i.e. B_0^2, B_0^4, B_4^4, B_0^6, and B_4^6 (B_0^2, B_0^4, B_3^4, B_0^6, B_3^6, and B_6^6). The c.f. parameters were obtained by a least squares fitting procedure between the experimental and calculated energy level values by minimizing the mean square deviation σ [16].

The strength of the c.f. interaction was evaluated by using the strength S [17] and relative strength S^k ($k = 2$, 4, and 6) [18] parameters, which are defined as follows:

$$S = \left\{ \frac{1}{3} \sum_k \frac{1}{2k+1} \left[(B_0^k)^2 + 2 \sum_{q>0} ((B_q^k)^2 + (S_q^k)^2) \right] \right\}^{1/2}, \tag{3}$$

$$S^k = \left[(B_0^k)^2 + 2 \sum_{q>0} (B_q^k)^2 \right]^{1/2}, \tag{4}$$

S and S^k can be used as a quantitative measure of the crystal field in a particular host [17,19]. It also provides a useful quantity to measure the c.f. strength between different matrices. The S^2, S^4, and S^6 are called as the long-, mid-, and short-range c.f. strength parameters [18], respectively, which may connect these quantities to the spatial extension of the c.f. effect.

3.2. Interpretation of spectroscopic data

The $4f^3$ configuration of the Nd^{3+} ion consists of 182 doubly degenerate Stark levels (Kramer doublets). The number of the Stark levels for a particular free ion $^{2S+1}L_J$ state is $J + 1/2$ for any symmetry lower than cubic. For both the C_{4v} and C_{3v} site symmetry the ground state $^4I_{9/2}$ should split into five Stark levels. According to the group theoretical selection rules, transitions between all Stark levels are allowed as both electric and magnetic dipole transitions [20]. The ground state splitting of NdOF was resolved by the INS technique at 2.5 K. All four transitions from the lowest Stark level were observed (0, 14, 130, 161, and 645 cm^{-1}) [12].

The absorption spectra of the stoichiometric NdOF were characterized by intense absorption bands near 350, 520, and 580 nm. The observed levels represent well the energy level scheme of Nd^{3+} below 34500 cm^{-1} without the interference of the host lattice. The analysis of the optical absorption and luminescence spectra yielded 117 Stark levels [21, 22].

In the NdOCl case, the ground state was resolved by the luminescence from the LaOCl matrix using powder samples at 9 K. All Stark levels were resolved (0, 90, 120, 268, and 339 cm^{-1}). The other 101 Stark levels were resolved by the optical absorption using either single crystal or powder samples [11]. The analysis of the optical spectra of NdOCl (both luminescence and absorption) yielded 106 Stark levels.

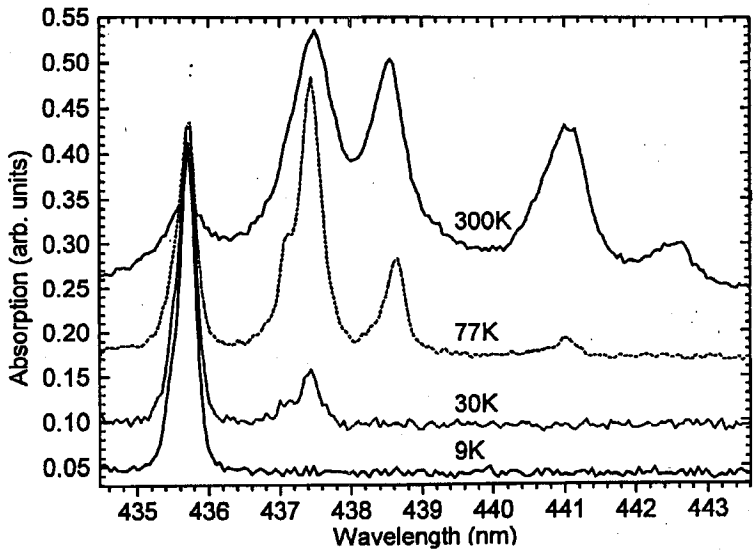

Fig. 1. The absorption from the $^4I_{9/2}$ state to the $^2P_{1/2}$ state in the NdOBr matrix at the temperatures of 9, 30, 77, and 300 K.

The experimental data for NdOBr were obtained by the absorption spectroscopy alone. Using the hot band absorption from the $^4I_{9/2}$ state, the energies of five Stark levels (0, 91, 151, 275, and 359 cm^{-1}) were confirmed (Fig. 1). At 9 K, 93 Stark levels were resolved. The large band absorption, due to the activator–host lattice interaction, was observed near 230 nm which energy is higher than the one observed for NdOF (*ca.* 36000 cm^{-1}).

4. Discussion

The spectroscopic measurements yielded 122, 105, and 98 Stark levels out of the theoretical 182 for NdOF, NdOCl, and NdOBr, respectively. The observed energy levels give basic sets sufficient enough for reliable energy level simulations. A model with 19 (or 20) parameters including 14 free ion (Racah, Trees, and

Judd parameters, as well as spin–orbit coupling constant) and five (or six) c.f. parameters was used for NdOX (X = Cl and Br) (and NdOF). In the case of NdOBr, the Judd parameters were left with fixed values. The simulations were carried out down to satisfactory root mean square (rms) deviations 17, 20, and 19 cm^{-1} for NdOF, NdOCl, and NdOBr, respectively.

4.1. Free ion interaction

Since the barycenters of the c.f. multiplets, i.e. the $^{2S+1}L_J$ states, do not change from one host lattice to another, the free ion parameters should assume similar values in the three NdOX matrices [23]. Some differences were observed, however. The Racah parameters show clear trends (Table) (presented in Fig. 2 as the Slater integrals F^k (k = 2, 4, and 6) [23]). The F^2 value decreases and the F^4 one increases as a function of the increasing ionic radius of the anion in the NdOX series. The F^6 value shows less clear trend. The spin–orbit interaction is constant in the series but the interconfigurational terms, i.e. the Trees and Judd parameters, show no clear trends. In general, the parameters are well defined with low estimated standard deviations, but the simulation of the energy level scheme of NdOBr cannot be considered as a final one.

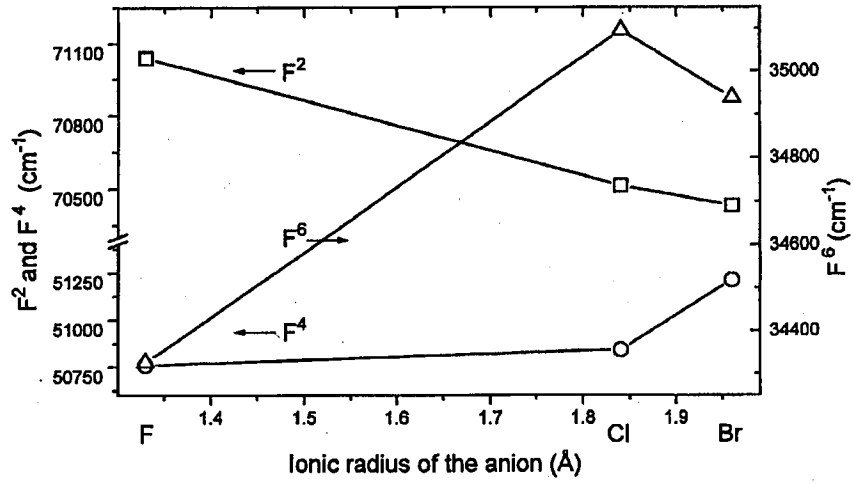

Fig. 2. The evolution of the Slater integrals F^k (k = 2, 4, and 6) in the NdOX (X = F, Cl, and Br) series as a function of the ionic radius of the anion.

4.2. Nephelauxetic effect

With increasing covalency the interaction between the $4f$ electrons is reduced, since the electrons are delocalized. While the electronic repulsion is reduced, the energy separation between different energy levels decreases. This phenomena is called as the nephelauxetic (= cloud expanding) effect [1, 24, 25]. This effect can

be studied in terms of both the positions of the individual $^{2S+1}L_J$ states [24] and by the nephelauxetic parameter β [26], which is the ratio between the electron repulsion terms in the solid state and in the free ion.

TABLE

The free ion, c.f. strength, and nephelauxetic parameters (cm^{-1}) in the NdOX series (X = F, Cl, and Br).

Parameter	NdOF	NdOCl [11]	NdOBr
E_0	23429(1)	11616(36)	23248(2)
E_2	4689(1)	4697(7)	4696(8)
E_4	23.17(1)	22.92(4)	22.89(1)
E_6	477.95(8)	471.20(15)	471.56(8)
α	21.62(3)	19.6(3)	20.40(3)
β	-625(3)	-649(12)	-667(4)
γ	1880(4)	1791(29)	1809(5)
T^2	424(2)	398(38)	[397][a]
T^3	52(2)	32(4)	[31][a]
T^4	55(2)	75(5)	[75][a]
T^6	-282(5)	-240(11)	[-248][a]
T^7	379(7)	296(22)	[322][a]
T^8	312(7)	330(26)	[338][a]
ζ_{4f}	870(1)	870(2)	870(1)
B_0^2	144(15)	-920(19)	-953(10)
B_0^4	1839(27)	-333(54)	-374(32)
B_3^4	-1643(17)		
B_4^4		-819(36)	862(21)
B_0^6	1005(31)	934(47)	888(26)
B_3^6	866(21)		
B_4^6		-209(45)	190(27)
B_6^6	812(22)		
S	650	367	377
S^4	2324	1206	1276
S^6	1956	976	92[illegible]
β^b	0.69417	0.6896	0.6888
σ	17	20	19
No. of levels	122/182	105/182	98/182

[a]The values in brackets were not varied freely but fixed close to the values of NdOCl.
[b]The nephelauxetic parameter
$\beta = F^2(\text{crystal})/F^2(\text{free ion})$ [26].

The evolution of the electron repulsion is described by the Racah parameters (Table) or Slater integrals (Fig. 2). A decrease in these parameters can be interpreted as an expansion of the $4f$ electron cloud. The F^2 parameter is the one most affected by the environment and it provides the best measure of covalence. The β parameter can then be expressed as the ratio between the F^2 parameters, $\beta = F^2(\text{crystal})/F^2(\text{free ion})$ [27]. The free ion F^2 values were obtained by the Dirac–Fock method [28]. A low β value indicates an important delocalization of the $4f$ electrons on the ligands and hence a significant covalent character in bonding [27]. In general, the values of β vary along the nephelauxetic series: $F^- > Cl^- > Br^-$ [26]. In the neodymium oxyhalide series, NdOBr has the smallest and NdOF the largest β value as expected, $\beta(F^-) = 0.6942$, $\beta(Cl^-) = 0.6896$, and $\beta(Br^-) = 0.6888$ (Table). An alternative way to evaluate the nephelauxetic effect

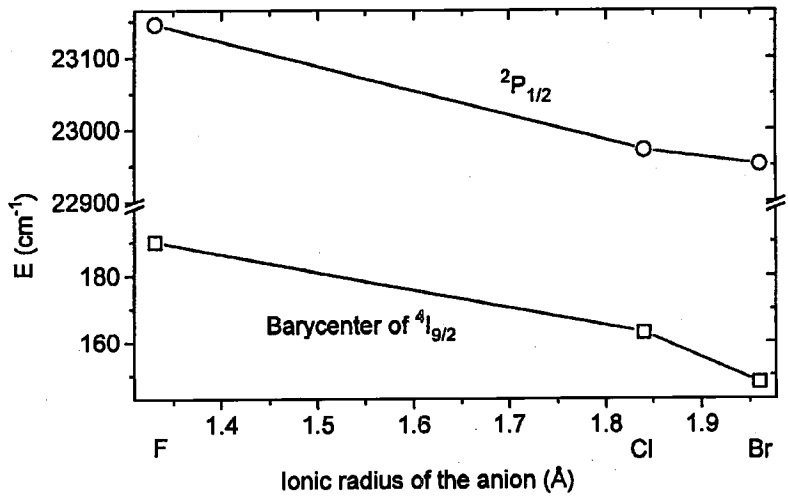

Fig. 3. The variation of the energy of the $^2P_{1/2}$ state and the barycenter of the ground state $^4I_{9/2}$ in the NdOX (X = F, Cl, and Br) series.

is to compare the energy positions of the individual $^{2S+1}L_J$ states in different matrices [24]. If one of the Slater integrals decreases, or all of them, the barycenter of the individual $^{2S+1}L_J$ states will lower [25]. The $^2P_{1/2}$ state of the Nd^{3+} ion at 23000 cm^{-1} is isolated and observed as one line in the spectra, therefore it is useful for this comparison. In the NdOX series, the energy of the $^2P_{1/2}$ state as well as the energy of the barycenter of the ground state $^4I_{9/2}$ decreases as a function of the increasing ionic radius of the anion (Fig. 3). The variation of the energy is not completely regular, since the experimental data is obtained by different methods, but the observations agree with the conclusions made from the Slater integrals.

4.3. Crystal field effect

The comparison of the individual c.f. parameters is difficult, since the site symmetry of the RE^{3+} ion differs in the NdOX series. The c.f. parameters are

affected by the distances, bonding angles, and the nature of ligands which characterize the crystallographic site of the RE^{3+} ion [25]. The value of B_0^2 describing the long-range c.f. interaction differs the most and is much larger in the tetragonal NdOCl and NdOBr matrices than in the trigonal NdOF (Table). The value of the axial short-range (sixth-rank) B_0^6 parameter decreases as a function of the increasing ionic radius, but as a whole, the fourth- and sixth-rank parameters are best treated in terms of the relative c.f. strength S^k (Eq. (4)) and the overall c.f. strength S (Eq. (3)) parameters (Fig. 4). The long-range c.f. strength S^2 is only the absolute value of B_0^2 which increases from NdOF to NdOBr. The evolution of the mid- and long-range c.f. strength parameters is reverse to that of S^2 and shows similar behavior as the overall c.f. parameter S.

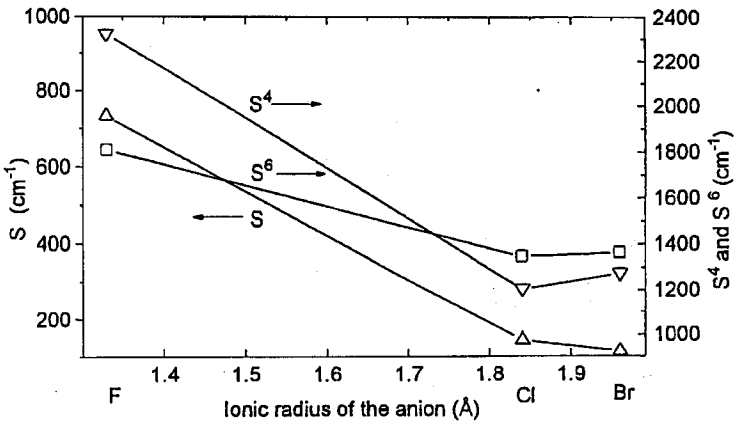

Fig. 4. The evolution of the c.f. strength S and the relative strength S^k ($k = 4$ and 6) parameters in the NdOX (X = F, Cl, and Br) series.

In the NdOF matrix, the main contribution to the c.f. strength comes from the mid- and short-range c.f. effects (Table), which indicate important electrostatic interaction between the cation and the electronegative anions O^{2-} and F^-. Since in the case of tetragonal oxyhalides (NdOCl and NdOBr), the significance of the long-range c.f. effect increases and S^4 as well as S^6 decrease, the importance of the electrostatic interaction lowers and the other effects, i.e. covalence, become more remarkable. This is in agreement with reduction observed in the F^2 parameter. The covalence correlates positively with this reduction as follows: free ion $< F^- < O^{2-} < Cl^- < Br^-$ which anti-correlates with the spectrochemical series which orders the ligands according to the relative magnitude of their c.f. contributions [29]. Thus, the ionicity is the predominant contribution to the c.f. effect.

5. Conclusions

The complete energy level scheme of the Nd^{3+} ion in different oxyhalide matrices were simulated by using the basis set of energy level values obtained by

the optical absorption and luminescence as well as the inelastic neutron scattering techniques. The analysis yielded 122, 105, and 98 Stark levels for NdOF, NdOCl, and NdOBr, respectively. The energy level schemes were successfully simulated according to the C_{3v} and C_{4v} site symmetries by a phenomenological model resulting in an rms deviation of 17 to 20 cm^{-1}.

The values of the Slater integral F^2, which is the most sensitive to the environment, indicates that the $4f$ electron cloud is more expanded in NdOBr than in NdOCl and NdOF. The former indicates that the Coulomb interaction is the weakest in the oxybromide matrix.

The c.f. effect — measured as the c.f. strength (S) — is almost twice as strong in the trigonal NdOF than in the tetragonal NdOCl and NdOBr. The decreasing c.f. strength and energy of the Stark levels together with the decreasing electron repulsion indicated the increasing nephelauxetic effect and covalence from NdOF to NdOBr. The same was observed in the variation of the nephelauxetic parameter, $\beta = F^2(\text{solid})/F^2(\text{free ion})$, which assumed the smallest value in NdOBr and the largest in NdOF.

Acknowledgments

The authors are indebted to Prof. M. Godlewski from the Institute of Physics, Polish Academy of Science, Warsaw, Poland, for the use of the luminescence equipment and Dr. H. Mutka from the Institut Max von Laue – Paul Langevin, Grenoble, France, for the INS measurements. Financial support from the Academy of Finland (project No. 4966) and the Ministry of Education to J.H., J.K., R.-J.L, H.R., and E.S. is gratefully acknowledged.

References

[1] G. Blasse, B.C. Grabmaier, *Luminescence Materials*, Springer Verlag, Berlin 1994.

[2] D. Garcia, M. Faucher, in: *Handbook on the Physics and Chemistry of Rare Earths*, Vol. 21, Eds. K.A. Gschneidner, Jr., L. Eyring, Elsevier, Amsterdam 1995, p. 263.

[3] C.L. Li, M. Reid, *Phys. Rev. B* **42**, 1903 (1990).

[4] P. Porcher, P. Caro, *J. Less-Common Met.* **93**, 151 (1983).

[5] P. Caro, *J. Less-Common Met.* **16**, 367 (1968).

[6] *Int. Tabl. Crystallogr.*, Eds. N.F.M. Henry, K. Lonsdale, Vol. 1, Kynoch Press, Birmingham 1969.

[7] A.W. Mann, D.J. Bevan, *Acta Crystallogr. B* **26**, 2129 (1970).

[8] L.H. Brixner, E.P. Moore, *Acta Crystallogr. C* **39**, 1316 (1983).

[9] J. Hölsä, P. Porcher, *J. Chem. Phys.* **75**, 2108 (1981).

[10] J. Hölsä, P. Porcher, *J. Chem. Phys.* **76**, 2790 (1982).

[11] L. Beaury, Ph.D. Thesis, Université de Paris-Sud, Orsay 1988.

[12] E. Hölsä, J. Säilynoja, L. Beaury, J. Derouet, P. Porcher, O. Antson, H. Mutka, *Inorg. Chem.*, 1996, in press.

[13] B.G. Wybourne, *Spectroscopic Properties of Rare Earths*, Interscience, New York 1965.

[14] H. Crosswhite, H.M. Crosswhite, B.R. Judd, *Phys. Rev.* **169**, 11 (1979).

[15] P. Porcher, *Phase Transit.* **12**, 233 (1988).

[16] P. Porcher, *Computer Programs Reel and Image for the Simulation of d^N and f^N Configurations Involving the Real and Complex Crystal Field Parameters*, C.N.R.S., Meudon 1989, unpublished.

[17] N.C. Chang, J.B. Gruber, R.P. Leavitt, C.A. Morrison, *J. Chem. Phys.* **76**, 3877 (1982).

[18] T.A. Metcalf, D.H. Hopkins, F.S. Richardson, *Inorg. Chem.* **34**, 4868 (1995).

[19] F. Auzel, *Mater. Res. Bull.* **14**, 223 (1979).

[20] J.L. Prather, *Monograph 19*, US National Bureau of Standards, Washington, 1961.

[21] E. Säilynoja, Ph.D. Thesis, University of Turku, Turku 1996.

[22] E. Antic-Fidancev, J. Hölsä, P. Porcher, E. Säilynoja, 1996, unpublished.

[23] S. Hüfner, *Optical Spectra of Transparent Rare Earth Compounds*, Academic Press, London 1978.

[24] E. Antic-Fidancev, M. Lemaitre-Blaise, P. Caro, *New J. Chem.* **11**, 467 (1987).

[25] P. Caro, J. Derouet, *Bull. Soc. Chim. Fr.* **1**, 46 (1972).

[26] J.-C. Krupa, *J. All. Comp.* **225**, 1 (1995).

[27] D.F. Shriver, P.W. Atkins, C.H. Langford, *Inorganic Chemistry*, Oxford University Press, Oxford 1990.

[28] A.J. Freeman, J.P. Desclaux, *J. Magn. Magn. Mater.* **12**, 11 (1979).

[29] D.J. Newman, B. Ng, Y.M. Poon, *J. Phys. C, Solid State Phys.* **17**, 5577 (1984).